Journal of Applied Mechanics and Technical Physics, Vol. 36, No. 1, 1995

MATHEMATICAL MODELS AND TOPOLOGICAL METHODS IN WING AERODYNAMICS

S. K. Betyaev and O. P. Brysov

UDC 532.527

The current level of exactitude of order-of-magnitude estimation in hydrodynamics is based on extensive use of the asymptotic methods. Thus, in wing theory the Reynolds number Re is traditionally considered to be a large parameter, since, on one hand, in aviation it reaches values of 10^7 to 10^8, and, on the other hand, it is only this simplifying assumption that opens the way to mathematical modeling of the problem, specifically the use of the basically asymptotic Prandtl concept of the inviscid nature of the flow on the scales of the wing chord or wing span.

Topological Methods. The unconventional dependences (obtainable with the aid of tunnel experimentation) of the integral and distributed aerodynamic characteristics on the angle of attack continue to amaze investigators with their hysteresis, spontaneously arising asymmetry, spirality, nonstationarity, and so on. Being a "black box," such an experiment does not make it possible to clarify the nature of the phenomenon. Various versions regarding the nature of the phenomenon and the flow schemes (topology) — and this means the mathematical models of the flow around the wing — are constructed on the basis of qualitative experimentation, with the aid of which, specifically, we can determine the topological properties of the isolines (usually the streamlines) on the surface of the wing or on the flow symmetry plane [1].

Since $Re >> 1$, we need to differentiate the field of the surface friction lines (limiting streamlines) right on the wing and the field of the surface streamlines of the inviscid flow at the outer edge of the boundary layer. The topography of the former is usually determined by the oil dot method, the topography of the latter is determined by the tuft method or by visualizing the near-wall stream filaments using an injectable dye.

We note that in experimental aerodynamics the topographic methods determine an average (in time) field of the surface lines and therefore are suitable when the nonstationarity is small.

We introduce on the plane stream surface the rectangular x, y coordinate system and denote the corresponding velocity components by u and v, and we direct the velocity component w that is normal to the plane along the z axis. Away from the vicinity of the separation line, we have from the nonpenetration condition $w(x, y, z) = zw_0(x, y) + o(z)$. The potential of the laminar incompressible fluid flow is now determined not from the three-dimensional Laplace equation but rather from the two-dimensional Poisson equation with unknown right side $(-w_0)$. Therefore we can not obtain complete information on the flow on the stream surface without solving the problem as a whole.

The inviscid flow surface streamlines are the trajectories of the ordinary differential equation

$$\frac{dy}{dx} = \frac{v}{u}.$$

Their topology is determined by the type and location of the singular points: $u = v = 0$. The surface streamline field is nonsolenoidal, since we have from the continuity equation

$$\frac{\partial u(x, y)}{\partial x} + \frac{\partial v(x, y)}{\partial y} = -w_0(x, y).$$

The nonsolenoidality of the surface streamline field indicates the possibility of the appearance of node-type singular points. We examine the solution in the vicinity of the singular point $x = y = 0$, assuming that the first derivatives of the velocity and the vorticity are finite. Then the normal to the surface $z = 0$ component of the vorticity vector in this vicinity is constant and equal

Zhukovskii. Translated from Prikladnaya Mekhanika i Tekhnicheskaya Fizika, No. 1, pp. 40-47, January-February, 1995. Original article submitted January 4, 1994; revised March 10, 1994.

0021-8944/95/3601-0038$12.50

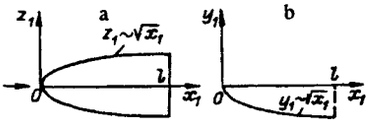

Fig. 1

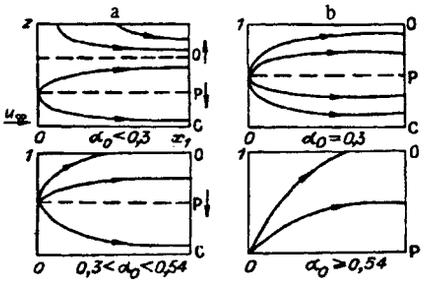

Fig. 2

to $u_y - v_x$. We find from the vorticity transport equation, which reduces to the single-term condition of the absence of stretching and rotation of the vortex lines $(u_y - v_x)A = 0$, where $A = w_0(0, 0)$, that in the three-dimensional motion ($A \neq 0$) the normal component of the vorticity is equal to zero, i.e., $u_y = v_x$. The singular point of the equation of the surface streamlines is a saddle if $u_y^2 - u_x v_y > 0$ and is a node if $u_y^2 - u_x v_y > 0$.

Thus, in the framework of the adopted assumption on finiteness of the derivatives there are no focus-type singular points. This conclusion is valid if the plane $z = 0$ is a plane of symmetry. If the plane $z = 0$ is the surface of the wing, then, as experiment shows, focal singularities arise. Their appearance is apparently explained by the separated nature of the flow, and this means by violation of the condition of finiteness of the gradient of the velocity or the vorticity.

In accordance with the no-slip condition, the projection of the viscous fluid flow velocity on the wing is proportional to z or z^2. The field of the viscous fluid streamlines on the wing surface are the trajectories of the ordinary differential equation

$$\frac{dy}{dx} = \frac{\partial v/\partial z}{\partial u/\partial z}\Big|_{z=0}.$$

Since the Navier–Stokes equation is of higher order than the Euler equation, no limitations on the coefficients of the expansions of the velocity components in integer powers of z can be obtained from the N–S equation. Consequently, singularities of any types are possible in the flow of a viscous fluid, specifically at the base of the boundary layer [2, 3].

In the general case no direct connection has been established between the singularities at the base of the boundary layer and at its outer edge; they may be of different types and may be spaced at a finite distance from one another, defining two topologically different near-wall flow fields. The situation is disrupted when the vorticity extends from the depths of the boundary layer into the outer inviscid region. Thus, in the case of tornado-like separation a focal singularity is characteristic for both near-wall flow fields.

Asymptotic Wing Theory. The flow around a wing depends on at least five principal dimensionless parameters: the aspect ratio λ, the free stream Mach number M_∞, the angle of attack α, the maximal relative wing thickness δ, and the Reynolds number Re. This large number of parameters makes the problem unsolvable, and further idealization is required for the construction of the mathematical model. We shall start from the tail end of this list of parameters. We have already defined the value of Re as a large parameter, thereby converting to the Euler equations. The wing thickness is usually small, and its influence is considered to be linear everywhere except in the vicinity of the edges of the wing, where it is necessary to introduce a special expansion. Therefore, setting $\delta = 0$, we shall consider the wing surface to be plane.

In connection with the broadening of the operational range of the angles of attack of the modern airplanes and missiles clear up to 180°, the quantity α can take two values: $\alpha = 0(1)$ and $\alpha << 1$. In the first case the flow around the wing is subsonic if $M_\infty < 1$, and supersonic if $M_\infty > 1$. In the second case the classification of the regimes is more complex: $M_\infty < 1$) — subsonic linear theory, $(M_\infty - 1)\alpha^{-2/3} = O(1)$ — transonic theory, $M_\infty > 1$ — supersonic linear theory, $M_\infty \alpha = O(1)$ — hypersonic theory.

In asymptotic wing theory the only remaining parameter, which we have not yet dealt with, λ, is considered to be either large or small. In both approximations the vicinity of the wing is a narrow inner zone, in which the law of plane sections is valid: in the plane that is normal to the longitudinal coordinate of the zone the three-dimensional flow is equivalent to plane flow.

Accordingly, we differentiate: wing profile theory ($\lambda = \infty$), high aspect ratio wing theory ($\lambda >> 1$), finite aspect ratio wing theory ($\lambda = 0(1)$), and low aspect ratio wing theory ($\lambda << 1$).

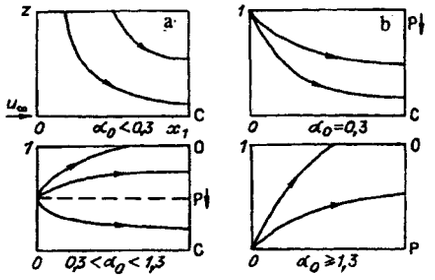

Fig. 3

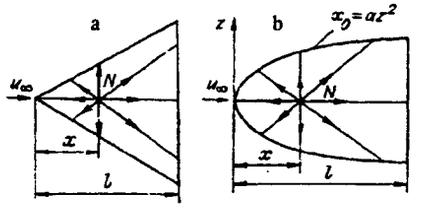

Fig. 4

In the framework of high aspect ratio wing theory there have been constructed mathematical models of subsonic flow [4] and transonic flow [5], and also of planing flow. The topology of the streamlines is trivial everywhere except for the side edges of the wing, since in the inner region, the scale of which is equal to the wing chord, the law of plane sections holds: the wing profiles are subject to flow independently of one another.

In the theory of the wing of low aspect ratio there have been constructed mathematical models of subsonic, transonic, supersonic, and hypersonic flow around the wing, the model of the flow around the side edge of the rectangular [6, 7], and also the model of the flow around an elongated ship [8]. In the case of subsonic or supersonic flow in the inner region, the scale of which is equal to the wing span, for $\alpha >> \lambda$ the stationary analogy with plane flow is valid: the wing cross sections are subject to flow independently of one another; for $\alpha = 0(1)$ the nonstationary analogy with plane flow is valid: the longitudinal coordinate plays the role of time [9, 10]. With account for flow separation from the side edges, we obtain the nontrivial topological patterns of the flow around the wing of low aspect ratio. An example of this pattern can be constructed if we use the unsteady analogy with plane flow and the exact solution of the plane problem in the so-called Nikol'skii flow case [11]. In accordance with the unsteady analogy, to the plane problem of the flow around a flat plate, traveling and expanding with a velocity that is proportional to $t^{-1/2}$ (t is the time), there corresponds the flow around a wing of low aspect ratio that is parabolically curved in planform (Fig. 1a) and in the plane of symmetry (Fig. 1b). The side edges of this wing are curved in accordance with the law

$$z_1 = \lambda l \left(\frac{x_1}{l}\right)^{1/2},$$

and the centerline has the form

$$y_1 = -\alpha_0 \lambda l \left(\frac{x_1}{l}\right)^{1/2} < 0,$$

where l is the wing length; $\lambda << 1$ is the aspect ratio; $\alpha_0 = 0(1)$ is the relative angle of attack.

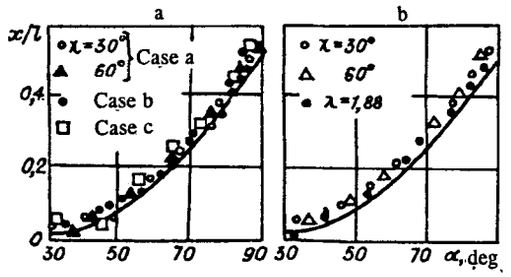

Fig. 5

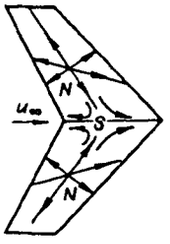

Fig. 6

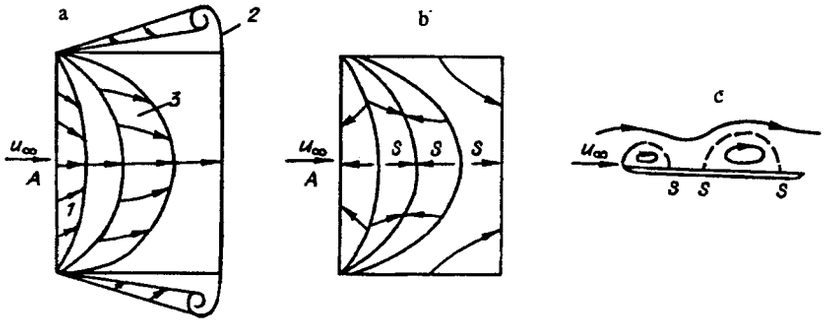

Fig. 7

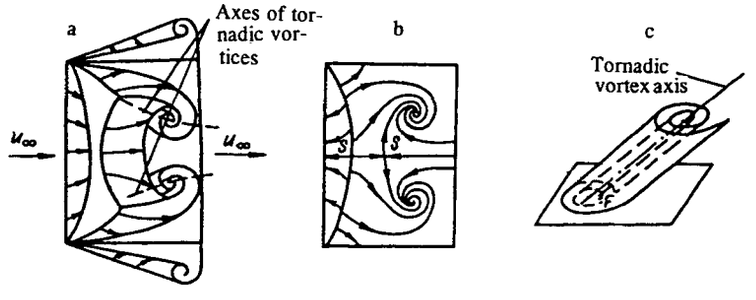

Fig. 8

In the variables x_1 and

$$z = \frac{z_1}{\lambda l}\left(\frac{x_1}{l}\right)^{-1/2}$$

the wing becomes "rectangular": $|z| \leq 1$, $x_1 > 0$. Figure 2 demonstrates the streamline field on the upper surface of the wing as a function of α_0, Fig. 3 shows the field on the lower surface. The topology changes for $\alpha_0 \simeq 0.3$, 0.54, and 1.3. The line of symmetry $z = 0$ may be either a line of flow spreading (P) or a line of flow confluence (C). The arrows on the surface streamlines indicate the direction of the relative velocity vector. The vertical arrows indicate the direction of motion of the singular points with increase of α_0. A saddle-type singular point corresponds to the line of flow convergence in the plane self-similar flow, and a node-type singular point corresponds to the line of flow spreading. In the Nikol'skii solution the line of flow separation (0) is degenerate, and the velocity on this line is continuous. Therefore the line of flow separation coincides with the singular line (line of flow confluence).

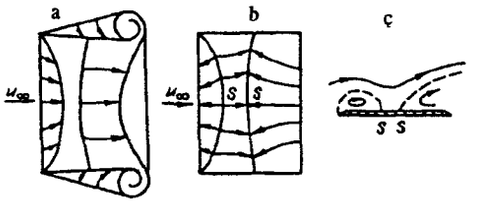

Fig. 9

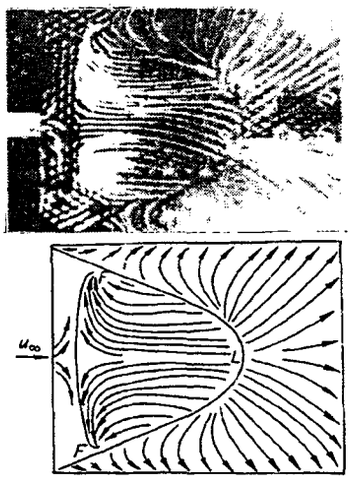

Fig. 10

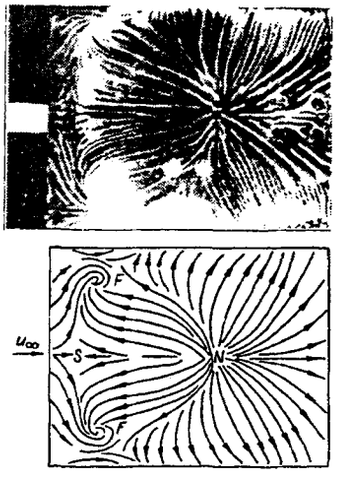

Fig. 11

Linear theories for both subsonic flow [12] and supersonic flow [13, 14] have been developed for the thin wings of finite aspect ratio that are positioned at a small angle of attack. The linear theories do not describe the singularities in the streamline field.

Fundamental events take place on the upper surface of the wing of finite aspect ratio. We shall examine the behavior of the surface friction lines on the upper surface later, here we shall restrict ourselves to a discussion of the topological pattern of the flow past the lower surface of the wing of finite aspect ratio, which differs fundamentally from the pattern of the flow past the lower surface of the wing of low aspect ratio. In the case being examined for the traditional wing planforms the field of the surface streamlines contains only one singular point — a node N. The flow topology is shown schematically in Fig. 4a, b, respectively, for a triangular wing and a parabolic wing ($x_0 = az^2$).

The dependence of the node position x/l on the model angle of attack α was determined experimentally in the TsAGI GT-1 water tunnel ($Re \simeq 2 \cdot 10^4$) and in the TsAGI T-03 wind tunnel ($Re \simeq 5.2 \cdot 10^5$).

In the water tunnel we tested five models with base width b = 80 mm: a) triangular wings with sweep angles $\chi = 30$ and 60°; b) parabolic wings of length $l = 15$ and 25 mm; c) a rectangular wing of length $l = 30$ mm. The dependence of x/l on α is shown in Fig. 5a. The solid curve is the relation calculated using the Rayleigh formula

$$\frac{x}{l} = \frac{2\cos\alpha(1 + \sin^2\alpha) + (\pi - \alpha)\sin\alpha + 2}{\pi\sin\alpha + 4},$$

which corresponds to the flow around a rectangular wing of infinite span (flat plate) following the Helmholtz scheme. The agreement of the experimental data and this simple theory is satisfactory. Moreover, the dependence of x/l on α is universal — it is the same for all the wing planforms.

It is considered that the Helmholtz scheme is suitable only for the flow of a liquid and is not applicable for the flow of a compressible gas. To determine the dependence of x/l on α in a compressible gas, experiments were performed in the T-03 subsonic wind tunnel at low speeds ($M_\infty = 0.1$). We tested two triangular wing models with apex angle 30 and 60 degrees,

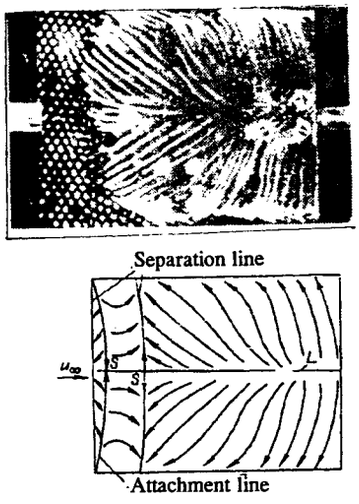

Fig. 12

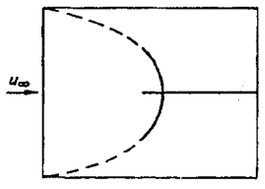

Fig. 13

and also a rectangular wing model with aspect ratio 1.88. The dependence of x/l on α for these models is compared with the Rayleigh curve in Fig. 5b. Satisfactory agreement is again observed.

Thus, the position of the nodal singularity on the lower surface of the wing is independent of both the wing planform and the properties of the moving continuum. We note that this law may not hold, for example, for the wing with reverse sweep, the assumed scheme of the flow around which with two nodes N and a saddle S is shown in Fig. 6.

Flow around a Rectangular Wing. The asymptotic theory is valid when the parameter λ is small ($\lambda << 1$) or large ($\lambda >> 1$), but is invalid otherwise. The aerodynamics of the wing of finite aspect ratio that is set at a finite angle of attack, i.e., the region $\alpha = O(\lambda) = O(1)$ — is the realm of experiment [15-17] and computational hydrodynamics [18, 19]. A mathematical model of the flow around a wing of finite aspect ratio that is applicable in the entire angle-of-attack variation range has not yet been constructed, since this flow is accompanied by phenomena that are too complex. Of inestimable assistance in constructing the mathematical model is a qualitative experiment, as a result of which there is established the flow topology that is necessary both for the verification of the numerical methods and for the development of the mathematical submodels describing the local properties of the flow.

We studied in the T-03 wind tunnel with the aid of the oil dot method the pattern of the surface friction lines on the upper surface of a rectangular wing with chord 110 mm and aspect ratio 1.82. The wing was a flat plate with sharp edges. Three topologically different flow regimes were discovered.

In the first regime, along with the spiral separation 2 from the side edges and the bubble-like separation from the leading edge 1 (leading-edge bubble), at small angles of attack there was observed a primary bubble 3 (Fig. 7a). Figure 7, a-c show the lines at the outer edge of the bubbles, the field of the surface friction lines, and the flow in the plane of symmetry AA.

With increase of the angle of attack α to about 17° the primary bubble expands, the line of flow attachment reaches the wing trailing edge, and, splitting, forms two tornado-like [tornadic] vortices (Fig. 8a), the initiators of which are two focal singularities in the surface friction lines (Fig. 8b). Figure 8c shows the three-dimensional tornado-like vortex sheet.

The third regime is realized when $\alpha > 25°$. The tornado-like vortices break down, as the angle of attack approaches 90° the extensive leading-edge separation tends to occupy the entire upper surface of the wing, and the separation from the side edges becomes unsteady and multi-spiral (Fig. 9).

The Psi-effect. The flow around the wing with aspect ratio $\lambda < 1$ is characterized by greater topological diversity than the flow around the wing with $\lambda > 1$. We studied in the T-03 wind tunnel two rectangular wing models: 1) $\lambda = 0.5$, chord 180 mm, span 90 mm; 2) $\lambda = 0.8$, chord 150 mm, span 120 mm.

When the angles of attack are small, the flow regime does not differ from that shown in Fig 7. With increase of the angle of attack, the primary bubble grows in size, with its ends remaining at the front corners of the wing, and the line of flow attachment moves toward the trailing edge. Then the growth of the primary bubble terminates and the flow separation zone breaks down, to which there corresponds the formation at $\alpha \simeq 28°$ of two focal singularities F, shown in Fig. 10 (in Figs.

10-12 the upper diagrams are the photographs of the oil tracks, the lower diagrams are the corresponding maps of the friction lines). With increase of the angle of attack, the line of flow spreading L, located on the normal to the line of symmetry, contracts, degenerating at $\alpha \simeq 38°$ to a point — the node N, indicated in Fig. 11. It follows from the Poincaré principle that a saddle point will be located near each focus in this figure. However we were not able to reliably detect these saddle singularities in the experiments.

This is the topology of the flow around the wing with $\lambda = 0.5$. For the wing with $\lambda = 0.8$ the foci and the node appear practically simultaneously at an angle of attack $\alpha \simeq 28°$.

Further increase of the angle of inclination of the wing to the approaching flow leads to a situation in which there appears a line of flow spreading that is located on the axis of symmetry of the model (Fig. 12). The tail of this line finally reaches the edge of the wing. Then the separated zone that is adjacent to the wing leading edge expands; the regime of complete separation develops, bypassing (at least for the wing with $\lambda = 0.5$) the stage that is shown in Fig. 9.

The locus of the ends of the line of flow spreading describes as a function of α a curve in the form of a recumbent letter ψ (Fig. 13). This is the source of the name for this phenomenon — the psi-effect.

At the present time the tornado-like vortex is being studied using computational methods [19], therefore it is desirable to perform a numerical verification of all the topological regimes of the flow around wings and, in particular, the psi-effect.

The authors wish to thank A. P. Gordienko and T. Yu. Gracheva for their assistance in performing the experiments.

REFERENCES

1. H. K. Moffatt and A. Tsinober (eds.), Topological Fluid Mechanics, Cambr. Univ. Press, Cambridge (1990).
2. D. Yu. Shevelev, Three-Dimensional Problems of Computational Aerohydrodynamics [in Russian], Nauka, Moscow (1986).
3. E. H. Hirschel and W. Kordulla, Shear Flow of a Compressible Fluid [Russian translation], Mir, Moscow (1987).
4. M. Van-Dyke, Perturbation Methods in Fluid Mechanics [Russian translation], Mir, Moscow (1967).
5. J. D. Cole and L. P. Cook, Transonic Aerodynamics [Russian translation], Mir, Moscow (1987).
6. H. K. Cheng, "Aerodynamics of a rectangular plate with vortex separation in supersonic flow," J. of the Aeronautical Sciences, **22**, No. 4, pp. 217-226 (1955).
7. V. F. Molchanov, "Method of identification of the principal part of the nonlinear characteristics of a rectangular wing in ideal fluid flow," Uchen. Zap. TsAGI, **11**, No. 1, pp. 12-17 (1980).
8. J. N. Newman, Marine Hydrodynamics [Russian translation], Sudostroenie, Leningrad (1985).
9. A. A. Nikol'skii, "Similarity laws for three-dimensional steady separated liquid and gas flow around bodies," Uchen. Zap. TsAGI, **1**, No. 1, pp. 1-7 (1970).
10. S. K. Betyaev, "Mathematical modeling of laminar flows," Moscow (1994). Deposited at VIMI, No. DO-8567.
11. A. A. Nikol'skii, S. K. Betyaev, and I. P. Malyshev, "On the limiting form of separated self-similar ideal fluid flow," in: Problems of Applied Mathematics and Mechanics [in Russian], pp. 262-268, Nauka, Moscow (1971).
12. G. G. Chernyi, Gas Dynamics [in Russian], Nauka, Moscow (1988).
13. E. A. Krasil'shchikova, The Thin Wing in Compressible Flow [in Russian], Nauka, Moscow (1978).
14. J. W. Miles, Potential Theory of Unsteady Supersonic Flows [Russian translation], GIFML, Moscow (1963).
15. W. Stahl and M. Mahmood, "Some aspects of the flow past a square flat plate at high incidence," Z. Flugwiss. Weltraumforsch., **3**, No. 9, pp. 134-142 (1985).
16. G. Gregoriou, "Modern missile design for high angle-of-attack," AGARD-LS-121, pp. 5.1-5.23 (1982).
17. A. Winkelmann, "Flow visualization studies of the tip vortex system of a semi-infinite wing," AIAA Paper No. 1801 (1989).
18. B. Hunt, "The role of computational fluid dynamics in high angle-of-attack aerodynamics," AGARD-LS-121, pp. 6.1-6.28 (1987).
19. C. A. J. Fletcher, Computational Techniques for Fluid Dynamics [Russian translation], Vol. 1, Mir, Moscow (1991).